Journal of Affective Disorders Reports 14 (2023) 100641

Contents lists available at ScienceDirect

Journal of Affective Disorders Reports

journal homepage: www.sciencedirect.com/journal/journal-of-affective-disorders-reports

Research Paper

Linking resting state metabolite concentrations in the dorsal anterior cingulate cortex to response inhibition in OCD, a combined fMRI-MRS study

Niels T. de Joode [a,b,*], Anders L. Thorsen [c,d], Chris Vriend [a,b], Petra J.W. Pouwels [e], Anton J.L.M. van Balkom [f], Kristen Hagen [c,g], Olga T. Ousdal [c,h,i], Bjarne Hansen [c,d], Gerd Kvale [c,j], Odile A. van den Heuvel [a,b,c]

[a] Amsterdam UMC, Vrije Universiteit Amsterdam, Dept. Psychiatry, Dept. Anatomy and Neurosciences, Amsterdam De Boelelaan 1117, Amsterdam, Netherlands
[b] Amsterdam Neuroscience, Compulsivity Impulsivity Attention program, Amsterdam, Netherlands
[c] Bergen Center for Brain Plasticity, Haukeland University Hospital, Bergen, Norway
[d] Center for Crisis Psychology, University of Bergen, Bergen, Norway
[e] Amsterdam UMC, Vrije Universiteit Amsterdam, Radiology and Nuclear medicine, Amsterdam Neuroscience, De Boelelaan 1117, Amsterdam, Netherlands
[f] GGZ inGeest Specialised Mental Health Care, Amsterdam, The Netherlands
[g] Psychiatric Department, Hospital of Molde, Molde, Norway
[h] Department of Radiology, Haukeland University Hospital, Bergen, Norway
[i] Department of Biomedicine, University of Bergen, Bergen, Norway
[j] Department of Clinical Psychology, University of Bergen, Bergen, Norway

ARTICLE INFO

Keywords:
1H-MRS
fMRI
glutamate+glutamine (Glx)
obsessive-compulsive disorder
response Inhibition
Stop signal task

ABSTRACT

Introduction: Obsessive-compulsive disorder (OCD) has been associated with abnormal brain activation in regions related to response inhibition, such as the dorsal anterior cingulate cortex (dACC), as well as dysregulation of the glutamate system. We studied how the neurometabolites glutamate and glutamine (Glx) in the dACC are related to task performance and task-related brain activation during a response inhibition task in OCD patients and healthy controls (HC).

Methods: We combined resting-state magnetic resonance spectroscopy (1H-MRS) in the dACC and functional MRI (fMRI) during the Stop Signal Task (SST), using data from two sites (43 OCD patients and 41 HC). For fMRI data, region of interest (ROI) and whole brain analyses were performed during successful inhibition and error processing. Subsequently, the relation between baseline Glx concentrations, task-related activation, functional connectivity, and task performance was tested using correlational analyses.

Results: In HC, Glx concentration in dACC showed a positive correlation with inhibition-related activation in the right thalamus (based on ROI analyses) and the brain stem (based on whole brain analyses). No relation between Glx and task-related activation was observed in patients with OCD. SST performance was not different between groups and was not associated with dACC Glx concentrations.

Limitations: Although we attempted to link neurometabolite levels and brain activation, the non-simultaneous acquisition of 1H-MRS with fMRI made it difficult to interpret the results.

Conclusions: We conclude that dACC Glx is associated with inhibition-related activation and network function in HC, but not in OCD, suggesting altered inhibition processing in OCD.

Abbreviations: 1H-MRS, Proton magnetic resonance spectroscopy; BAI, Beck Anxiety Inventory; BDI, Beck Depression Inventory; CSTC, cortico-striato-thalamo-cortical; DSM-IV, Diagnostic and Statistical Manual of Mental Disorders, Fourth Edition; dACC, dorsal anterior cingulate cortex; FoV, Field of View; GAD-7, Generalized Anxiety Disorder; Glx, glutamate + glutamine; HC, Healthy Controls; IFG, inferior frontal gyrus; MRI, Magnetic Resonance Imaging; NAA, N-acetylaspartate; OCD, Obsessive-compulsive disorder; OCI-R, Obsessive-Compulsive Inventory-Revised; PHQ-9, Patient Health Questionnaire; pre-SMA, pre-supplemental motor area; PRESS, Point Resolved Spectroscopy; SST, stop signal task; SSRT, Stop-Signal Reaction Time; tCr, creatine + phosphocreatine; TE, Echo Time; tNAA, N-acetyl-aspartyl-glutamate+N-acetyl-aspartate; TR, Repetition Time; Y-BOCS, Yale-Brown Obsessive Compulsive Scale.

* Corresponding author
E-mail address: n.dejoode@amsterdamumc.nl (N.T. de Joode).

https://doi.org/10.1016/j.jadr.2023.100641
Received 30 June 2023; Received in revised form 28 July 2023; Accepted 3 August 2023
Available online 6 August 2023

1. Introduction

Inhibitory control is necessary to respond flexibly to changing demands and adequately suppress inappropriate or unwanted behavior. Obsessive compulsive disorder (OCD) is characterized by lower performance and altered brain activation in regions involved in response inhibition relative to healthy controls (HC), on tasks probing response inhibition (Abramovitch et al., 2013; de Wit et al., 2012; Norman et al., 2019). However, how altered performance and activation patterns relate to underlying neurometabolite levels is still unclear.

OCD is associated with abnormal function within and between the parallel cortico-striato-thalamo-cortical (CSTC), fronto-parietal, and fronto-limbic circuits (Stein et al., 2019; van den Heuvel et al., 2016). Within these circuits, the dorsal anterior cingulate cortex (dACC), inferior frontal gyrus (IFG), and pre-supplemental motor area (pre-SMA) serve important roles in error processing and cognitive/motor control (de Wit et al., 2012; Maltby et al., 2005; Marsh et al., 2014; McGovern and Sheth, 2017; Thorsen et al., 2018). Neuroimaging studies in OCD have shown hypoactivation of the dACC, IFG, and inferior parietal cortex and hyperactivation of the pre-SMA during successful inhibition (de Wit et al., 2012; Fitzgerald et al., 2005; Norman et al., 2019). During failed inhibition (error processing) hyperactivation of the dACC and pre-SMA is seen (de Wit et al., 2012; Fitzgerald et al., 2005; Norman et al., 2019).

The cortical regions involved in response inhibition are rich in glutamatergic projections, and dysregulation in glutamate signaling is proposed to contribute to OCD (Pittenger et al., 2011). Proton magnetic resonance spectroscopy (1H-MRS) studies have shown regional alterations in glutamate + glutamine (Glx) concentrations in OCD patients compared to healthy controls (HC), but the differences are often subtle and inconsistent between studies (Vester et al., 2020). Inconsistencies in 1H-MRS findings might be explained by variability in medication use, comorbidities, disease chronicity and severity, as well as differences in imaging parameters and voxel placement.

Although glutamate signaling has been proposed to play a role in OCD (Pittenger et al., 2011), the relation between brain activation and glutamatergic levels during inhibitory control is unknown. A better understanding between brain activation, glutamatergic levels, and task performance may provide important insight into the neurobiology of OCD, and may have implications for treatment (Goodman et al., 2021).

Previous studies found some evidence for a link between neurometabolite levels and brain activation during tasks and at rest in OCD patients and HC (Chen et al., 2019; Falkenberg et al., 2012; Yucel et al., 2007). In a group of HC, lower dACC glutamate levels were associated with stronger activation in the orbitofrontal cortex, inferior parietal cortex, and basal ganglia during an auditory cognitive control task, similar to a dichotic listening task (Falkenberg et al., 2012). In another study, Yücel and colleagues found that inhibition-related activation in de dACC during an interference task correlated negatively with N-acetylaspartate (NAA) levels in OCD patients, whereas HC did not show this correlation. Chen et al. (2019) studied the link between thalamic glutamate levels and resting state functional connectivity in OCD patients and HC (Chen et al., 2019). Altered functional connectivity between the thalamus and multiple frontal regions (including the dACC and SMA) was observed in OCD compared to HC. The thalamus-dACC connectivity at rest correlated negatively with thalamic glutamate levels in patients, but not in HC (Chen et al., 2019). In addition, multiple studies observed that Glx levels were proportionally related to the strength of the BOLD response in regions that receive glutamatergic projection from the region wherein Glx is measured (Duncan et al., 2014; Falkenberg et al., 2012; van Wageningen et al., 2010). The observed link between neurometabolite levels and (task-related) brain functioning validates the study on the relation between dACC Glx levels and inhibition-related activation in the predominantly glutamatergic connected CSTC and fronto-parietal regions to understand the role of glutamate in impaired inhibitory control in OCD.

In this study, we investigated how Glx (Glutamate + Glutamine) levels in the dACC are related to task performance, task-related activation and connectivity during inhibitory control and error processing in OCD patients and HC. To do so, we combined data of two European sites and harmonized data processing and analyses according to a preregistered analysis plan (https://osf.io/wdsrj). 1H-MRS data acquired during rest in the dACC was combined with whole brain task-based functional MRI (fMRI) while subjects performed the stop signal task (SST). This allowed us to investigate the relation between dACC Glx concentrations and task-related activation as well as functional connectivity during successful and failed inhibition. For all analyses, we investigated the relationship in the whole sample and subsequently for the OCD and HC groups separately. Based on previous literature, we expected task performance, measured as the stop signal reaction time (SSRT), to be negatively associated with dACC Glx for both patients and controls. We expected dACC Glx to be positively associated with inhibition-related BOLD responses in anterior insula, IFG and inferior parietal cortex and negatively associated with BOLD responses in the dACC during error processing. Finally, we expected functional connectivity during inhibition and error processing to be related to dACC Glx concentrations.

2. Experimental procedures

2.1. Participants

Data was pooled from two previously conducted studies in Amsterdam (The Netherlands) and Bergen (Norway), which resulted in a sample of 55 OCD patients and 53 HC. For the Bergen OCD sample, patients were recruited from a specialized outpatient OCD clinic at Haukeland University Hospital, Bergen, Norway. The Dutch OCD sample consisted of re-invited patients that were part of a previously assessed OCD cohort (de Wit et al., 2012). In Norway, HC were recruited through advertisements; in The Netherlands, HC were re-invited after taking part in previous studies. Patients were 18 years or older, had a primary diagnosis of OCD and were fluent Dutch or Norwegian. All participants had to be without MRI contraindications and major neurological illnesses. Other exclusion criteria were bipolar disorder or psychosis, intellectual disability, or substance abuse. Patients with comorbid anxiety or mood disorders were not excluded. HC had no lifetime history of any psychiatric disorder. Demographical and clinical characteristics for the separate samples and combined sample can be found in Table 2 and S1. Both studies were approved by their respective ethical committees (Amsterdam: ethical review board of VU university medical center, Bergen: The regional ethics committee for South-Eastern Norway). All participants provided informed written consent. The study was performed in accordance with the Declaration of Helsinki.

2.2. Clinical measures

All participants were diagnosed using the Structured Clinical Interview for DSM-IV (First et al., 2002). Severity of obsessive-compulsive symptoms was assessed in patients using the Y-BOCS (Goodman et al., 1989). Obsessive thought and compulsive behaviors were assessed in both patients and HC using the Obsessive-Compulsive Inventory-Revised (OCI-R) (Foa et al., 2002). In the Dutch sample, anxiety and depressive symptoms were measured using the Beck Anxiety Inventory (BAI) (Beck et al., 1988) and Beck Depression Inventory (BDI) (Beck et al., 1996), respectively, while the Generalized Anxiety Disorder (GAD-7) (Spitzer et al., 2006) and Patient Health Questionnaire (PHQ-9) (Kroenke et al., 2001) were used in Norway.

Since both sites used different clinical measures to assess depressive and anxious symptom severity, we converted the continuous BDI, BAI, PHQ-9, and GAD-7 scores in to categorical values (‘minimal’, ‘mild’, ‘moderate’, ‘severe’) based on established cut-offs.

2.3. Stop signal task

The SST consisted of go-trials that were pseudo-randomly mixed with stop-trials, with an 80/20 ratio (240 trials in total) (de Wit et al., 2012). During go-trials, participants had to respond to the direction of an arrow (left or right) depicted on the screen by pressing a button with their corresponding index finger. During stop-trials, a cross appeared over the presented arrow signaling that participants had to inhibit their initiated response. The cross appeared with a variable delay that adapted to the participants performance using a staircase tracking mechanism to reach roughly 50% successful stops. The stop-signal reaction time (SSRT) for each subject was calculated using the integration method in adherence with Verbruggen and colleagues (Verbruggen et al., 2019). Participants with a go-trial accuracy below 60% or failed stop-trials outside of the 25-75% range were excluded (Congdon et al., 2012).

2.4. Image acquisition

At both sites, MRI scans were performed on 3T General Electric Discovery MR750 (GE Healthcare, Milwaukee, Wisconsin, USA) with an eight-channel head coil. Both scan protocols included a structural T1-weighted image to aid individual voxel placement and to serve for brain segmentation based partial volume correction. In Amsterdam a 3D T1-weighted image was acquired with 172 slices, voxel size=1mm^3, echo time (TE)=3 ms, repetition time (TR)=7.8 ms, flip angle=12°, field of view (FoV)=256 × 256 mm (Fan et al., 2017). In Bergen the T1-weighted image was acquired with 192 slices, voxel size=1 mm^3, TE=30 ms, TR=7000 ms, flip angle=12°, FoV=256 × 256 mm. Both sites acquired 430 echo planar image volumes using a 64 × 64 matrix, 40 slices (Amsterdam), 34 slices (Bergen), (2.8 mm thickness with 0.2 mm gap), TR=2100 ms, TE=30 ms, flip angle=80°, $FoV_{Amsterdam}$=240 mm, FoV_{Bergen}=220, voxel $size_{Amsterdam}$=3.75 × 3.75 × 3 mm, voxel $size_{Bergen}$=3.44 × 3.44 × 3 mm. Single voxel MRS was conducted using a point resolved spectroscopy (PRESS) sequence (Amsterdam: TR=3000 ms, TE=35 ms, number of averages=64, voxel size=16 × 16 × 25 mm^3, number of data points=4096; Bergen: TR=1500 ms, TE=35 ms, number of averages=128, voxel size=16 × 20 × 24 mm^3, number of data points=4096). The MRS voxel was placed parallel to the frontal part of the midline corpus callosum on the dACC (Figure S1) (Dou et al., 2013).

2.5. Preprocessing of MR data and analyses

2.5.1. Spectral quantification and quality control

MRS spectra were fitted using LCModel with water scaling (Provencher, 1993) to obtain brain water referenced Glx concentrations from the dACC. Registration of structural scans and corresponding voxels was done using FSL FLIRT (Jenkinson and Smith, 2001). The structural MRI scan was segmented into grey matter (GM), white matter (WM) and cerebral spinal fluid (CSF) using FSL FAST (Jenkinson and Smith, 2001). Next, partial volume correction was applied for accurate water referenced quantification of metabolite concentrations. The MRS spectra were fitted between 3.67 and 1.0 ppm to prevent the influence of spoiling artefacts. Voxel placement was visually inspected by registering the structural scans and corresponding voxels to standard space (MNI) for each participant. Participants were excluded according to the following spectral quality criteria: the linewidth (full width at half maximum; FWHM) ≥0.1 ppm, the signal-to-noise ratio (SNR) ≤12, and when Cramer-Rao lower bounds (CRLBs) for either Glx, total NAA, or total creatine ≥20%. Figure S2 presents a representative MRS spectrum analyzed using LCModel for reference purposes. The current study adhered to the recommendations for minimum reporting standards for MRS studies as outlined by Lin and colleagues (Lin et al., 2021) (Table S3).

2.5.2. Preprocessing and quality control of fMRI data

FMRI data was preprocessed using fMRIprep and smoothed in SPM12 with a 6mm FWHM kernel. First-level models included accurate go-trials, accurate stop-trials, and failed stop-trials as 0s events. We applied a high pass filter with a 128 second cut-off. The signal coverage was visually inspected and participants with movement exceeding one voxel (3 mm) were excluded from analysis.

2.5.3. Statistical analyses

We ran separate regression analyses in SPM for the successful inhibition (successful stop>successful go) and error processing (failed stop>successful stop) contrasts with dACC Glx levels included as regressor of interest, controlled for SSRT, site, sex and age. Whole brain results were restricted to binarized brain masks based on whole sample (OCD and HC) main effects of task (inhibition and error processing) derived from a previous meta-analysis (Norman et al., 2019). The statistical threshold for the current analyses was set at $p<0.05$ (FWE). We performed these analyses on the whole sample, and separately for HC and OCD patients.

In SPM, one-sample regression analyses were applied to investigate whether there was a correlation between BOLD response in the ROIs during successful inhibition and error processing and dACC Glx concentrations, while controlling for SSRT, site, sex, and age. Additionally, a two-sample regression analysis was conducted to explore possible differences between the OCD and HC groups in the correlation between Glx and BOLD activation. Sensitivity analyses were performed to investigate whether the associations between Glx and functional activation were influenced by medication use in OCD patients, by running separate models with and without medicated subjects.

Additionally we conducted exploratory analyses to assess the relation between dACC Glx concentrations and task-related functional connectivity during successful and failed inhibition with the dACC as seed region, using the generalized psychophysiological interaction toolbox (gPPI) (McLaren et al., 2012). The dACC seeds were defined as 10 mm spheres centered on peak activation during inhibition (Left MNI: -6, 36, 24; Right MNI: 8, 38, 28) or error processing (Left MNI: -8, 28, 30) in the main effects of the current sample. Task-related functional connectivity with the dACC seeds was restricted to predefined inhibition and error related brain regions (Norman et al., 2019). For the inhibition contrasts these ROIs were 10 mm spheres placed in the AI/IFG (Left MNI: -30, 22, 6; Right MNI: 36, 22, -2), pre-SMA (Left MNI: -14, 14, 66; Right MNI: 6, 18, 56), inferior parietal cortex (Left MNI: -30, -48, 40; Right MNI: 34, -56, 50), and thalamus (Left MNI: -4, -22, -2; Right MNI: 8, -22, -2). For the error contrast, functional connectivity with the dACC was restricted to the 10 mm sphere in the left pre-SMA (Left MNI: 2, 14, 64) (Table 1.). The gPPI models included the three task regressors, three PPI regressors, time course of the seed region, and six motion

Table 1
ROIs used for inhibition and error contrast for fMRI analyses

Region	Hemisphere	MNI coordinates (X, Y, Z)
Successful inhibition (SucStop > SucGo)		
Anterior insula/IFG	L	-30, 22, 6
Anterior insula/IFG	R	36, 22, -2
dACC	L	-6, 36, 24
dACC	R	8, 38, 28
Inferior parietal cortex	L	-30, -48, 40
Inferior parietal cortex	R	34, -56, 50
Pre-SMA	L	-14, 14, 66
Pre-SMA	R	6, 18, 56
Thalamus	L	-4, -22, -2
Thalamus	R	8, -22, -2
Failed inhibition (FailStop > SucStop)		
dACC	L	-8, 28, 30
Pre-SMA	midline	2, 14, 64

Abbreviations: dACC, dorsal anterior cingulate cortex; IFG, inferior frontal gyrus; L, left; R, right; SMA, Supplementary motor area.

parameters.

3. Results

3.1. Demographics and clinical characteristics

Fifty-three HC and 55 OCD patients completed the scan protocol. Of those subjects, 12 HC and 12 patients were excluded either due to poor SST performance (one control and one patient), poor MRS spectral quality (six HC and nine patients), or too much movement or low quality of fMRI data (five HC and two patients). This resulted in a sample of 41 HC and 43 patients for the final analyses. Eight of those patients were taking serotonin reuptake inhibitors (SRIs), one patient was taking SRIs in combination with an antipsychotic drug and one patient was taking methylphenidate.

The demographics and clinical characteristics of the sample are described in Table 2. There were no differences between OCD patients and HC concerning age, sex, and education level. OCD patients had significantly higher depression and anxiety severity and scored significantly higher on the OCI-R questionnaire. OCD patients from the Bergen sample had a significantly higher Y-BOCS score compared to the Amsterdam sample ($U(OCD_{Bergen}=29, OCD_{Amsterdam}=14)=30000$, $z=4.49$, $p<.001$). The demographics and clinical characteristics for patient and HC groups for both sites separately are provided in Table S1.

3.2. Task performance and 1H-MRS

We observed no significant group differences in SSRT ($t(82)=.94$, $d=.21$, $p=.35$) and go-trial reaction time ($U(N_{OCD}=43, N_{HC}=41)=984.5$, $z=0.92$, $p=0.36$) (Table 3). No significant differences between patients and HC were observed for Glx ($U(N_{OCD}=43, N_{HC}=41)=894$, $z=0.11$, $p=0.91$) or reference metabolites creatine + phosphocreatine (tCr) and N-acetyl-aspartyl-glutamate+N-acetyl-aspartate (tNAA), and 1H-MRS quality measures (Table 3) either. In both groups, SSRT did not correlate with dACC Glx levels (HC ($r(36)=.07$, $p=.66$), patients ($r(38)=-.084$, $p=.61$)). Behavioral and 1H-MRS measures for patient and HC groups for both sites separately are provided in Table S2.

Table 2
Demographics and clinical characteristic of sample

Characteristic	OCD patients N=43	Healthy controls N=41	*p*
Age (mean years ± SD)	34.22 ± 11.29	34.38 ± 11.97	0.84[a]
Sex			0.50[b]
Female, *N* (%)	29 (67)	24 (59)	
Education level, N (%)			0.13[b]
Secondary school	1 (2)	3 (7)	
High school	22 (52)	13 (32)	
Higher education	19 (45)	25 (61)	
Depression severity, N (%)			<0.001[b]
Minimal	10 (23)	37 (90)	
Mild	13 (30)	4 (10)	
Moderate	10 (23)	0 (0)	
Severe	9 (21)	0 (0)	
Anxiety severity, N (%)			<0.001[b]
Minimal	9 (21)	35 (86)	
Mild	8 (19)	6 (15)	
Moderate	11 (26)	0 (0)	
Severe	14 (33)	0 (0)	
OCI-R (mean ± SD)	25.93 ± 10.89	5.07 ± 6.02	<0.001[a]
Y-BOCS (mean ± SD)	22.74 ± 7.87	-	-
Comorbidities, *N* (%)			
Anxiety[*]	15 (35)	-	-
Mood[#]	11 (26)	-	-
Medication use, *N* (%)			
SRI	8 (19)	-	-
SRI + antipsychotic	1 (2)	-	-
Methylphenidate	1 (2)	-	-

Abbreviations: OCI-R, Obsessive Compulsive Inventory-Revised; SRI, serotonin reuptake inhibitor; Y-BOCS, Yale-Brown Obsessive Compulsive Scale.
[*] social anxiety disorder and or, generalized anxiety disorder, specific phobia, panic disorder, agoraphobia, posttraumatic stress disorder
[#] major depressive disorder or dysthymia
[a] Mann-Whitney U test
[b] Fisher's Exact Test

Table 3
Behavioral and 1H-MRS outcomes

	Healthy controls (mean ± SD)	OCD patients (mean ± SD)	*df*	*t/z*	*p*
SSRT	213.07 ± 42.24	204.66 ± 40.00	82	0.94	0.35[a]
Go-trial reaction time (ms)	528.36 ± 133.16	547.07 ± 119.28	82	0.92	0.36[b]
Glx	23.65 ± 4.52	23.67 ± 3.67	82	0.11	0.91[b]
CRLB Glx (%)	6.88 ± 1.22	6.71 ± 1.25	82	0.34	0.74[b]
tCr	10.21 ± 1.05	10.31 ± 1.10	82	0.45	0.66[a]
CRLB tCr (%)	2.93 ± 0.41	3.12 ± 0.43	82	2.11	0.04[b]
tNAA	14.71 ± 1.78	14.94 ± 1.52	82	0.60	0.55[b]
CRLB tNAA (%)	3.1 ± 0.41	3.16 ± 0.43	82	0.40	0.69[b]
FWHM (ppm)	0.034 ± 0.004	0.033 ± 0.005	82	0.71	0.48[b]
SNR	17.34 ± 2.60	17.58 ± 2.84	82	0.78	0.43[b]

Abbreviations: CRLB, Cramer-Rao Lower Bound; FWHM, Full width at half maximum; Glx, (glutamate + glutamine); ms, milliseconds; ppm, parts per million; SNR, Signal-to-noise ratio; SSRT, stop signal response time; tCr, total creatine (Creatine + Phosphocreatine; tNAA, (N-acetyl-aspartyl-glutamate + N-acetyl-aspartate)
[a] Independent t-test
[b] Mann-Whitney U test

3.3. Task-related brain activation in OCD and HC

When the analysis was restricted to the predefined ROIs, no differences between patients and HC were detected in the contrasts for successful inhibition and error processing. Whole brain results at an uncorrected threshold ($\alpha_{uncorr}=.001$) showed that patients, compared to HC, exhibited increased activation in the left angular gyrus (MNI -38, 48, 20, $t=3.86$, $p_{uncorr}<.001$) and right superior occipital cortex (MNI 26, -96, 12, $t=3.28$, $p_{uncorr}<.001$) during successful inhibition. HC showed more inhibition-related activation in the right pre-SMA (MNI 18, -2, 62, $t=3.24$, $p_{uncorr}<.001$) and left medial frontal gyrus (MNI -30, 48, 18, $t=3.42$, $p_{uncorr}<.001$) compared to patients. During error processing, OCD patients, compared to HC, showed more activation in left inferior frontal gyrus (MNI -50, 14, 4, $t=3.68$, $p_{uncorr}<.001$) and left SMA (MNI 14, 10, 64, $t=3.42$, $p_{uncorr}<.001$). When compared to patients, HC showed more error-related activation in the left inferior parietal cortex (MNI -28, 56, 36, $t=3.41$, $p_{uncorr}=.001$) and left medial frontal gyrus (MNI -4, 48, 48, $t=3.53$, $p_{uncorr}<.001$).

3.4. Relationship between whole-brain task-induced activation and Glx concentration

We then investigated the relation between Glx and task-related brain activation, based on the restricted binarized whole brain masks for task contrasts. When looking at the whole study population, irrespective of diagnosis, we observed a positive trend correlation between dACC Glx concentration and inhibition-related activation in the right insula (MNI 36, 22, -10, $k_e=38$, $t=4.16$, $p_{FWE}=.073$, $r=.29$). However, in OCD patients, there was no relation between Glx concentration in the dACC and inhibition-related brain activation. In HC, we found a positive correlation between Glx concentration and inhibition-related activation in the brain stem (MNI 10, -26, -16, $k_e=13$, $t=5.21$, $p_{FWE}=.013$, $r=.55$) (Fig. 1A). Neither OCD patients nor HC showed a correlation between dACC Glx concentration and error-related BOLD activation. Omitting the medicated patients from the analyses did not influence the results.

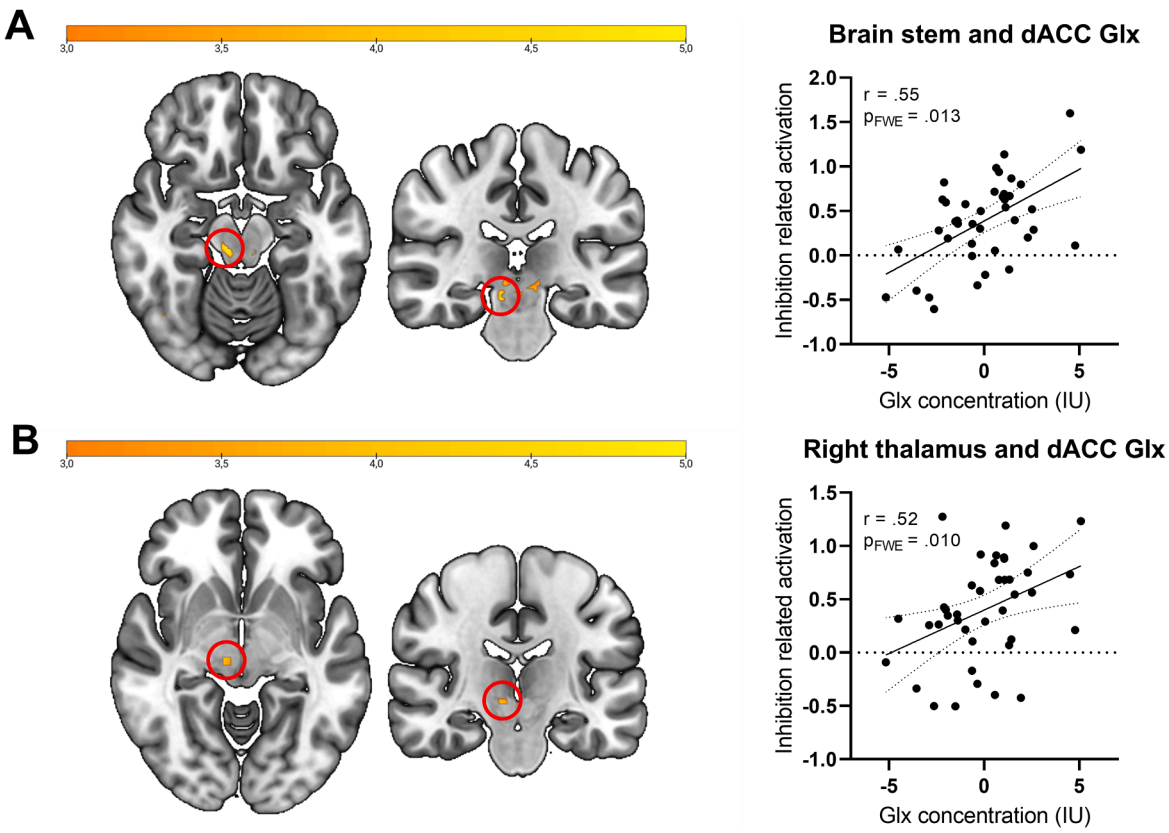

Fig. 1. Depiction of positive correlations of dACC Glx with task induced brain activation during successful inhibition contrast (successful STOP > successful GO) in healthy controls (n=41) in A) the right brain stem at the whole brain level and B) in the right thalamus when analyses were restricted to predefined ROIs. The left panels indicate the area were inhibition-related activation correlates with dACC Glx concentration on the MNI template. The panels on the right show the relation between extracted parameter estimates (controlled for site, sex, and Stop Signal Reaction Time) for the inhibition contrast and dACC Glx concentrations. Brain results are shown at a p_{uncorr}=.001 threshold for visualization purposes.

3.5. Relation Glx concentration with task-induced activation in ROIs

When restricting the correlation analyses to the predefined ROIs in Table 1, we observed a positive correlation between dACC Glx concentration and inhibition-related activation in the right insula/IFG ROI when looking at the whole sample (MNI 34, 22, -6, *k*=5, t=3.55, p_{FWE}=.030, r=.22). For patients, no association was seen between Glx concentration and inhibition-related activation. In HC, a positive correlation was found between dACC Glx concentration and inhibition-related activation in the right thalamus (MNI 10, -20, -6, ke=7, t=4.23, p_{FWE}=.010, r=.51) (Fig. 1B). There was no relationship between dACC and error-related activation for the whole sample, patients, or HC groups. The results were unaffected by removing the medicated patients from the analyses.

3.6. Relation Glx concentration with functional connectivity

There was no correlation detected between inhibition-related functional connectivity and dACC Glx levels in the whole sample. HC showed a negative correlation between dACC Glx concentration and connectivity between the right dACC and right pre-SMA, during successful inhibition (MNI 8, 14, 58, k_e=2, t=3.90, p_{FWE}=.029, r=-.40) (Fig. 2A). Additionally in HC, right dACC-right inferior parietal cortex connectivity was also negatively correlated with dACC Glx levels, however only at trend level (MNI 8, -54, 50, t=3.54, p_{FWE}=.067, r=-.39). Patients did not display any association between dACC Glx levels and functional connectivity during successful inhibition. When looking at error-processing, HC showed a positive correlation between dACC Glx and connectivity between the left dACC and right pre-SMA (MNI 4, 14, 66, *k*=44, t=3.76, p_{FWE}=.004, r=.42) (Fig. 2B). No relation between dACC Glx levels and dACC-seed functional connectivity was observed for the patient group and for analyses with and without medicated patients included.

4. Discussion

We studied the association between dACC Glx levels and inhibition and error-related brain activation and behavior in OCD patients and HC. Contrary to our hypothesis, we did not observe an association between SSRT and dACC Glx levels, but did observe a positive correlation between dACC Glx and right insular activation during inhibition in the whole sample. For HC, we did observe a positive relation between dACC Glx levels and inhibition-related activation in the brain stem, which was not seen in patients. When limiting our search area to predefined inhibition-related ROIs, HC, but not patients, showed a positive correlation between dACC Glx levels and inhibition-related activation in the thalamus. No association between dACC Glx levels and error-related brain activation was observed for patients or HC. In exploratory analyses we saw that in HC, but not in patients, Glx levels in the dACC correlated negatively with inhibition-related functional connectivity between the dACC and pre-SMA, while this correlation was positive during error processing. Summarizing, Glx concentrations in dACC are associated with inhibition-related network function in HC but not in OCD patients, suggesting altered mechanisms during inhibition and error-related processing.

We observed correlations between dACC Glx levels and inhibition-related activation in CSTC regions. Interestingly, no correlation between dACC Glx levels and task induced activation in the dACC itself

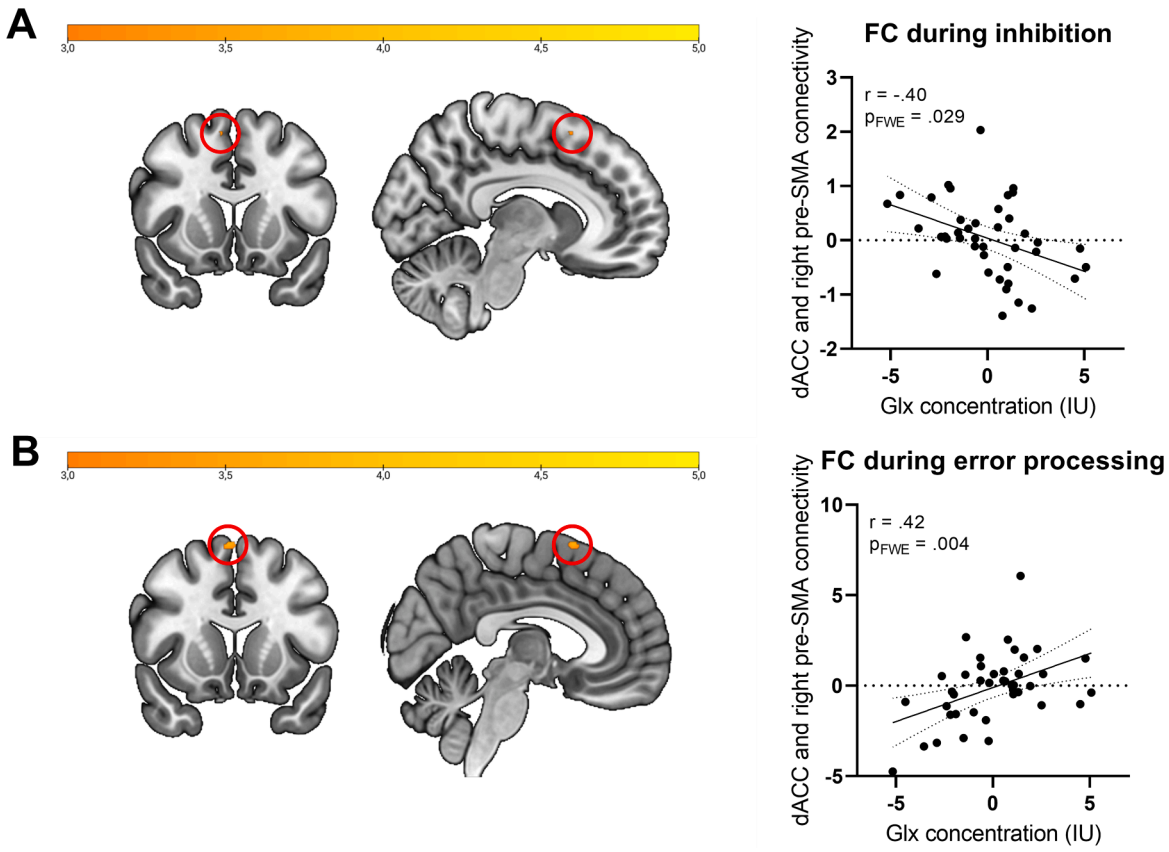

Fig. 2. Depiction of the relation between dACC Glx and functional connectivity between the dACC ROI seed and pre-SMA during A) successful inhibition (successful STOP > successful GO) and B) error processing contrasts (failed STOP > successful STOP) in healthy controls (n=41). The left panels indicate the area were dACC Glx levels are associated with dACC functional connectivity on a MNI template. The panels on the right show the relation between dACC-pre-SMA connectivity (controlled for site, sex, and Stop Signal Reaction Time) and dACC Glx concentrations. Brain results are shown at a p_{uncorr}=.001 threshold for visualization purposes.

was observed. This is in line with previous research indicating that Glx is proportionally related to the strength of the BOLD response in regions outside the region where Glx is measured (Duncan et al., 2014; Falkenberg et al., 2012; van Wageningen et al., 2010). We also found that dACC-preSMA functional connectivity correlated with dACC Glx levels in HC, but not patients. Both regions are involved in error monitoring and response inhibition and are connected through glutamatergic projections. Why this relation between functional connectivity and dACC Glx levels was observed to be opposite for the successful inhibition and error processing contrast is not clear and warrants further research.

The non-significant between-group difference in resting dACC Glx levels is in line with previous literature (Vester et al., 2020). Although previous studies have shown higher Glx concentrations in the cingulate cortex of OCD patients compared to HC, these alterations were mainly observed in the pregenual ACC rather than the dACC (de Salles Andrade et al., 2019; O'Neill et al., 2016). Future research could further elucidate potential Glx differences between the 'limbic' pregenual ACC versus the 'cognitive' dACC (Stein et al., 2019). The absence of Glx or glutamate baseline alterations in resting-state metabolite levels, despite the proposed role of altered glutamate signaling in OCD, suggests that simply comparing these metabolite levels at rest may not be adequate to study glutamatergic alterations in OCD. Recent studies indeed found that between-group differences in metabolite concentrations are subtle and are mainly observed in relation to clinical characteristics, behavioral performance, and task-induced states (de Joode et al., 2022; Yucel et al., 2007; Yucel et al., 2008). In line with this, we found that resting-state Glx levels correlated positively with inhibition-related activation in the thalamus and brain stem, but only in HC.

Although the brain stem was not included as ROI for the current study, we observed that the region was activated during inhibitory control in both HC and patients. Interestingly, Norman and colleagues observed similar brain stem activation of the brain stem during inhibition in their meta-analysis (Norman et al., 2019). The brain stem thus is important for response inhibition. The brainstem contains interesting nuclei like the locus coeruleus (LC), nucleus that produces noradrenaline, and substantia nigra (SN) and ventral tegmental area (VTA), nuclei that produce dopamine. These nuclei have widespread projections to (pre)frontal regions involved in response inhibition and modulate brain activation and glutamate transmission in these regions through catecholamine release (Aston-Jones and Cohen, 2005; Kohler et al., 2016). More specifically, the LC exerts an effect on other brain regions through tonic firing, related to arousal, and phasic firing related to attentional processes and task performance (Aston-Jones and Cohen, 2005; Howells et al., 2012). It is thought that increased tonic firing of the LC, which is observed in several animal models of anxiety as well as in patients with anxiety disorders, impairs phasic firing and thus hinders optimal performance (Howells et al., 2012; Kohler et al., 2016; Morris et al., 2020). We hypothesize that the absence of a correlation between dACC Glx levels and brain stem activation during successful inhibition in patients reflects a suboptimal interplay between the LC, dACC, and perhaps other regions involved in response inhibition and salience processing, such as preSMA and anterior insula/IFG (Chamberlain et al., 2006; Kohler et al., 2016; Minzenberg et al., 2008; Silvetti et al., 2018; van Velzen et al., 2014; van Wageningen et al., 2010). This remains speculative though, in the context of low spatial resolution when measuring LC activity using 3Tesla fMRI. Nevertheless, future studies could focus on pharmacological interventions targeting the glutamate system directly or indirectly through catecholamine modulation as potential new treatment strategies (Pittenger, 2015; van Velzen et al., 2014; van Wageningen et al., 2010).

4.1. Limitations

Some limitations of the study need to be addressed. Despite the fact that our two sites used similar scanners and harmonized image acquisition and data analysis, differences in 1H-MRS scan protocol (e.g. differences in voxel size and repetition time) do exist. This is reflected by between site differences in metabolite concentrations (Table S2). Although we controlled for site, these differences could introduce non-biological variability. In addition, different clinical scales were used to address depression and anxiety symptoms. We therefore converted the continuous measures to categorical values based on established cut-offs. Besides, we were not able to address clinical characteristics such as disease duration and medication load or history since information on these topics was absent or limited. Future studies could address both issues by the use software targeting potential site differences resulting from the use of multiple scanners such as ComBat and by the use of fully harmonized clinical protocols. Second, one of the samples included patients that were re-invited as part of a naturalistic follow-up from an earlier study (de Wit et al., 2012). When the scan session for the current study took place, patients experienced lower symptom severity often dipping below the clinical cut-off (Table S1). One could argue that if impaired response inhibition is dependent on symptom severity, it could explain why we do not observe differences in SST performance. It is however generally thought that impaired response inhibition is a trait or endophenotype of OCD that is not related to disease severity and is also reflected by inhibition-related brain activation in first degree unaffected siblings (de Wit et al., 2012; Lei et al., 2015; Lillevik Thorsen et al., 2020; Menzies et al., 2007). The notion that impaired response inhibition is a trait is strengthened by the absence of a relation between symptom severity and SSRT for our combined patient sample (data not shown) and the absence of a difference in SSRT between the two patient samples. Third, we tried to establish a link between neurometabolite concentrations and task induced brain activation. It should however be noted that we used static dACC Glx levels that were acquired within the same scan session, but not simultaneously with the fMRI acquisition. This makes interpretation of the link between Glx levels and inhibition-related brain activation difficult. Future research could more directly investigate the link between neurometabolites and brain activation during response inhibition in OCD by means of functional MRS (fMRS) interleaved with task-based fMRI at higher field strength (i.e. 7Tesla fMRS-fMRI) (Apšvalka et al., 2015; Bednarik et al., 2015; Stanley and Raz, 2018). Additionally, future studies could benefit from incorporating protocols that allow for reliable GABA measurements to capture both excitatory and inhibitory processes in the dACC and other regions relevant in the context of OCD and response inhibition (e.g. the pre-SMA).

4.2. Conclusions

In conclusion, we investigated the association between dACC Glx levels, task performance on the SST, and task-induced brain activation during successful and unsuccessful response inhibition in OCD patients and HC. In HC, but not OCD patients, dACC Glx concentrations correlated with inhibition-related activation in the brain stem and thalamus and with inhibition and error related connectivity between the dACC and pre-SMA. This indicates that dACC Glx is important for inhibition-related network function in health and suggests altered mechanisms underlying inhibition processing in OCD patients. Future research could more directly investigate the link between task induced brain activation and task induced neurometabolite concentrations using newly emerging imaging techniques, such as dynamic spectroscopy at higher field strength.

Author Disclosure

Contributors

Niels T. de Joode: conceptualization and design of the work; analysis and interpretation of data; writing the original draft; editing of intellectual content. Anders L. Thorsen: conceptualization and design of the work; acquisition, analysis and interpretation of data; writing the original draft; editing of intellectual content. Chris Vriend: conceptualization and design of the work; analysis and interpretation of data; writing the original draft; editing of intellectual content. Petra J.W. Pouwels: analysis and interpretation of data; editing of intellectual content. Anton J. L. M. van Balkom: conceptualization and design of the work; writing the original draft; editing of intellectual content. Kristen Hagen: acquisition and interpretation; editing of intellectual content. Olga T. Ousdal: acquisition and interpretation; editing of intellectual content. Bjarne Hansen: conceptualization and design of the work; analysis and interpretation of data; writing-original draft; editing of intellectual content; resources and funding acquisition. Gerd Kvale: conceptualization and design of the work; analysis and interpretation of data; writing-original draft; editing of intellectual content; resources and funding acquisition. Odile A. van den Heuvel: conceptualization and design of the work; analysis and interpretation of data; writing-original draft; editing of intellectual content; resources and funding acquisition.

Role of Funding Source

This study was supported by the Helse Vest Health Authority (Grant Nos. 911754 and 911880 [to GK]). ALT was supported by a travel grant from the Faculty of Psychology, University of Bergen, Bergen, Norway, when this work was carried out. NTdJ was paid by the VIDI grant from The Netherlands Organization for Health Research (ZonMw) to OAvdH (project number: 91717306).

Declaration of Competing Interest

The other authors report no biomedical financial interests or potential conflicts of interest.

Acknowledgements

None.

Supplementary materials

Supplementary material associated with this article can be found, in the online version, at doi:10.1016/j.jadr.2023.100641.

References

Abramovitch, A., Abramowitz, J.S., Mittelman, A., 2013. The neuropsychology of adult obsessive-compulsive disorder: a meta-analysis. Clin Psychol Rev 33, 1163–1171.
Apšvalka, D., Gadie, A., Clemence, M., Mullins, P.G., 2015. Event-related dynamics of glutamate and BOLD effects measured using functional magnetic resonance spectroscopy (fMRS) at 3 T in a repetition suppression paradigm. NeuroImage 118, 292–300.
Aston-Jones, G., Cohen, J.D., 2005. An integrative theory of locus coeruleus-norepinephrine function: adaptive gain and optimal performance. Annu Rev Neurosci 28, 403–450.
Beck, A.T., Epstein, N., Brown, G., Steer, R.A., 1988. An inventory for measuring clinical anxiety: psychometric properties. J Consult Clin Psychol 56, 893–897.
Beck, A.T., Steer, R.A., Ball, R., Ranieri, W., 1996. Comparison of Beck Depression Inventories -IA and -II in psychiatric outpatients. J Pers Assess 67, 588–597.
Bednarik, P., Tkac, I., Giove, F., DiNuzzo, M., Deelchand, D.K., Emir, U.E., Eberly, L.E., Mangia, S., 2015. Neurochemical and BOLD responses during neuronal activation measured in the human visual cortex at 7 Tesla. J Cereb Blood Flow Metab 35, 601–610.
Chamberlain, S.R., Muller, U., Blackwell, A.D., Clark, L., Robbins, T.W., Sahakian, B.J., 2006. Neurochemical modulation of response inhibition and probabilistic learning in humans. Science 311, 861–863.

Chen, Y., Meng, Z., Zhang, Z., Zhu, Y., Gao, R., Cao, X., Tan, L., Wang, Z., Zhang, H., Li, Y., Fan, Q., 2019. The right thalamic glutamate level correlates with functional connectivity with right dorsal anterior cingulate cortex/middle occipital gyrus in unmedicated obsessive-compulsive disorder: A combined fMRI and (1)H-MRS study. Aust N Z J Psychiatry 53, 207–218.
Congdon, E., Mumford, J.A., Cohen, J.R., Galvan, A., Canli, T., Poldrack, R.A., 2012. Measurement and reliability of response inhibition. Front Psychol 3, 37.
de Joode, N.T., Thorsen, A.L., Vester, E.L., Vriend, C., Pouwels, P.J.W., Hagen, K., Ousdal, O.T., Hansen, B., Kvale, G., van den Heuvel, O.A., 2022. Longitudinal changes in neurometabolite concentrations in the dorsal anterior cingulate cortex after concentrated exposure therapy for obsessive-compulsive disorder. J Affect Disord 299, 344–352.
de Salles Andrade, J.B., Ferreira, F.M., Suo, C., Yucel, M., Frydman, I., Monteiro, M., Vigne, P., Fontenelle, L.F., Tovar-Moll, F., 2019. An MRI Study of the Metabolic and Structural Abnormalities in Obsessive-Compulsive Disorder. Front Hum Neurosci 13, 186.
de Wit, S.J., de Vries, F.E., van der Werf, Y.D., Cath, D.C., Heslenfeld, D.J., Veltman, E. M., van Balkom, A.J., Veltman, D.J., van den Heuvel, O.A., 2012. Presupplementary motor area hyperactivity during response inhibition: a candidate endophenotype of obsessive-compulsive disorder. Am J Psychiatry 169, 1100–1108.
Dou, W., Palomero-Gallagher, N., van Tol, M.J., Kaufmann, J., Zhong, K., Bernstein, H. G., Heinze, H.J., Speck, O., Walter, M., 2013. Systematic regional variations of GABA, glutamine, and glutamate concentrations follow receptor fingerprints of human cingulate cortex. J Neurosci 33, 12698–12704.
Duncan, N.W., Wiebking, C., Northoff, G., 2014. Associations of regional GABA and glutamate with intrinsic and extrinsic neural activity in humans-a review of multimodal imaging studies. Neurosci Biobehav Rev 47, 36–52.
Falkenberg, L.E., Westerhausen, R., Specht, K., Hugdahl, K., 2012. Resting-state glutamate level in the anterior cingulate predicts blood-oxygen level-dependent response to cognitive control. Proc Natl Acad Sci U S A 109, 5069–5073.
Fan, S., Cath, D.C., van den Heuvel, O.A., van der Werf, Y.D., Schols, C., Veltman, D.J., Pouwels, P.J.W., 2017. Abnormalities in metabolite concentrations in tourette's disorder and obsessive-compulsive disorder-A proton magnetic resonance spectroscopy study. Psychoneuroendocrinology 77, 211–217.
First, M.B., Spitzer, R.L., Gibbon, M., Williams, J.B.W., 2002. Structured Clinical Interview for DSM-IV-TR axis I Disorders, research version, patient edition (SCID I/P). Biometrics Research, New York State Psychiatric Institute, New York, NY.
Fitzgerald, K.D., Welsh, R.C., Gehring, W.J., Abelson, J.L., Himle, J.A., Liberzon, I., Taylor, S.F., 2005. Error-related hyperactivity of the anterior cingulate cortex in obsessive-compulsive disorder. Biol Psychiatry 57, 287–294.
Foa, E.B., Huppert, J.D., Leiberg, S., Langner, R., Kichic, R., Hajcak, G., Salkovskis, P.M., 2002. The Obsessive-Compulsive Inventory: development and validation of a short version. Psychol Assess 14, 485–496.
Goodman, W.K., Price, L.H., Rasmussen, S.A., Mazure, C., Fleischmann, R.L., Hill, C.L., Heninger, G.R., Charney, D.S., 1989. The Yale-Brown Obsessive Compulsive Scale. I. Development, use, and reliability. Arch Gen Psychiatry 46, 1006–1011.
Goodman, W.K., Storch, E.A., Sheth, S.A., 2021. Harmonizing the Neurobiology and Treatment of Obsessive-Compulsive Disorder. Am J Psychiatry 178, 17–29.
Howells, F.M., Stein, D.J., Russell, V.A., 2012. Synergistic tonic and phasic activity of the locus coeruleus norepinephrine (LC-NE) arousal system is required for optimal attentional performance. Metab Brain Dis 27, 267–274.
Jenkinson, M., Smith, S., 2001. A global optimisation method for robust affine registration of brain images. Med Image Anal 5, 143–156.
Kohler, S., Bar, K.J., Wagner, G., 2016. Differential involvement of brainstem noradrenergic and midbrain dopaminergic nuclei in cognitive control. Hum Brain Mapp 37, 2305–2318.
Kroenke, K., Spitzer, R.L., Williams, J.B., 2001. The PHQ-9: validity of a brief depression severity measure. J Gen Intern Med 16, 606–613.
Lei, H., Zhu, X., Fan, J., Dong, J., Zhou, C., Zhang, X., Zhong, M., 2015. Is impaired response inhibition independent of symptom dimensions in obsessive-compulsive disorder? Evidence from ERPs. Sci Rep 5, 10413.
Lillevik Thorsen, A., de Wit, S.J., Hagland, P., Ousdal, O.T., Hansen, B., Hagen, K., Kvale, G., van den Heuvel, O.A., 2020. Stable inhibition-related inferior frontal hypoactivation and fronto-limbic hyperconnectivity in obsessive-compulsive disorder after concentrated exposure therapy. Neuroimage Clin 28, 102460.
Lin, A., Andronesi, O., Bogner, W., Choi, I.Y., Coello, E., Cudalbu, C., Juchem, C., Kemp, G.J., Kreis, R., Krssak, M., Lee, P., Maudsley, A.A., Meyerspeer, M., Mlynarik, V., Near, J., Oz, G., Peek, A.L., Puts, N.A., Ratai, E.M., Tkac, I., Mullins, P. G., Experts' Working Group on Reporting Standards for, M.R.S., 2021. Minimum Reporting Standards for in vivo Magnetic Resonance Spectroscopy (MRSinMRS): Experts' consensus recommendations. NMR Biomed 34, e4484.
Maltby, N., Tolin, D.F., Worhunsky, P., O'Keefe, T.M., Kiehl, K.A., 2005. Dysfunctional action monitoring hyperactivates frontal-striatal circuits in obsessive-compulsive disorder: an event-related fMRI study. Neuroimage 24, 495–503.
Marsh, R., Horga, G., Parashar, N., Wang, Z., Peterson, B.S., Simpson, H.B., 2014. Altered activation in fronto-striatal circuits during sequential processing of conflict in unmedicated adults with obsessive-compulsive disorder. Biol Psychiatry 75, 615–622.
McGovern, R.A., Sheth, S.A., 2017. Role of the dorsal anterior cingulate cortex in obsessive-compulsive disorder: converging evidence from cognitive neuroscience and psychiatric neurosurgery. J Neurosurg 126, 132–147.
McLaren, D.G., Ries, M.L., Xu, G., Johnson, S.C., 2012. A generalized form of context-dependent psychophysiological interactions (gPPI): a comparison to standard approaches. Neuroimage 61, 1277–1286.
Menzies, L., Achard, S., Chamberlain, S.R., Fineberg, N., Chen, C.H., del Campo, N., Sahakian, B.J., Robbins, T.W., Bullmore, E., 2007. Neurocognitive endophenotypes of obsessive-compulsive disorder. Brain 130, 3223–3236.
Minzenberg, M.J., Watrous, A.J., Yoon, J.H., Ursu, S., Carter, C.S., 2008. Modafinil shifts human locus coeruleus to low-tonic, high-phasic activity during functional MRI. Science 322, 1700–1702.
Morris, L.S., McCall, J.G., Charney, D.S., Murrough, J.W., 2020. The role of the locus coeruleus in the generation of pathological anxiety. Brain Neurosci Adv 4, 2398212820930321.
Norman, L.J., Taylor, S.F., Liu, Y., Radua, J., Chye, Y., De Wit, S.J., Huyser, C., Karahanoglu, F.I., Luks, T., Manoach, D., Mathews, C., Rubia, K., Suo, C., van den Heuvel, O.A., Yucel, M., Fitzgerald, K., 2019. Error Processing and Inhibitory Control in Obsessive-Compulsive Disorder: A Meta-analysis Using Statistical Parametric Maps. Biol Psychiatry 85, 713–725.
O'Neill, J., Lai, T.M., Sheen, C., Salgari, G.C., Ly, R., Armstrong, C., Chang, S., Levitt, J. G., Salamon, N., Alger, J.R., Feusner, J.D., 2016. Cingulate and thalamic metabolites in obsessive-compulsive disorder. Psychiatry Res Neuroimaging 254, 34–40.
Pittenger, C., 2015. Glutamatergic agents for OCD and related disorders. Curr Treat Options Psychiatry 2, 271–283.
Pittenger, C., Bloch, M.H., Williams, K., 2011. Glutamate abnormalities in obsessive compulsive disorder: neurobiology, pathophysiology, and treatment. Pharmacol Ther 132, 314–332.
Provencher, S.W., 1993. Estimation of metabolite concentrations from localized in vivo proton NMR spectra. Magn Reson Med 30, 672–679.
Silvetti, M., Vassena, E., Abrahamse, E., Verguts, T., 2018. Dorsal anterior cingulate-brainstem ensemble as a reinforcement meta-learner. PLoS Comput Biol 14, e1006370.
Spitzer, R.L., Kroenke, K., Williams, J.B., Lowe, B., 2006. A brief measure for assessing generalized anxiety disorder: the GAD-7. Arch Intern Med 166, 1092–1097.
Stanley, J.A., Raz, N., 2018. Functional Magnetic Resonance Spectroscopy: The "New" MRS for Cognitive Neuroscience and Psychiatry Research. Front Psychiatry 9, 76.
Stein, D.J., Costa, D.L.C., Lochner, C., Miguel, E.C., Reddy, Y.C.J., Shavitt, R.G., van den Heuvel, O.A., Simpson, H.B., 2019. Obsessive-compulsive disorder. Nat Rev Dis Primers 5, 52.
Thorsen, A.L., Hagland, P., Radua, J., Mataix-Cols, D., Kvale, G., Hansen, B., van den Heuvel, O.A., 2018. Emotional Processing in Obsessive-Compulsive Disorder: A Systematic Review and Meta-analysis of 25 Functional Neuroimaging Studies. Biol Psychiatry Cogn Neurosci Neuroimaging 3, 563–571.
van den Heuvel, O.A., van Wingen, G., Soriano-Mas, C., Alonso, P., Chamberlain, S.R., Nakamae, T., Denys, D., Goudriaan, A.E., Veltman, D.J., 2016. Brain circuitry of compulsivity. Eur Neuropsychopharmacol 26, 810–827.
van Velzen, L.S., Vriend, C., de Wit, S.J., van den Heuvel, O.A., 2014. Response inhibition and interference control in obsessive-compulsive spectrum disorders. Front Hum Neurosci 8, 419.
van Wageningen, H., Jorgensen, H.A., Specht, K., Hugdahl, K., 2010. A 1H-MR spectroscopy study of changes in glutamate and glutamine (Glx) concentrations in frontal spectra after administration of memantine. Cereb Cortex 20, 798–803.
Verbruggen, F., Aron, A.R., Band, G.P., Beste, C., Bissett, P.G., Brockett, A.T., Brown, J. W., Chamberlain, S.R., Chambers, C.D., Colonius, H., Colzato, L.S., Corneil, B.D., Coxon, J.P., Dupuis, A., Eagle, D.M., Garavan, H., Greenhouse, I., Heathcote, A., Huster, R.J., Jahfari, S., Kenemans, J.L., Leunissen, I., Li, C.R., Logan, G.D., Matzke, D., Morein-Zamir, S., Murthy, A., Pare, M., Poldrack, R.A., Ridderinkhof, K. R., Robbins, T.W., Roesch, M., Rubia, K., Schachar, R.J., Schall, J.D., Stock, A.K., Swann, N.C., Thakkar, K.N., van der Molen, M.W., Vermeylen, L., Vink, M., Wessel, J.R., Whelan, R., Zandbelt, B.B., Boehler, C.N., 2019. A consensus guide to capturing the ability to inhibit actions and impulsive behaviors in the stop-signal task. Elife 8.
Vester, E.L., de Joode, N.T., Vriend, C., Pouwels, P.J.W., van den Heuvel, O.A., 2020. Little evidence for neurometabolite alterations in obsessive-compulsive disorder - A systematic review of magnetic resonance spectroscopy studies at 3 Tesla. Journal of Obsessive-Compulsive and Related Disorders 25.
Yucel, M., Harrison, B.J., Wood, S.J., Fornito, A., Wellard, R.M., Pujol, J., Clarke, K., Phillips, M.L., Kyrios, M., Velakoulis, D., Pantelis, C., 2007. Functional and biochemical alterations of the medial frontal cortex in obsessive-compulsive disorder. Arch Gen Psychiatry 64, 946–955.
Yucel, M., Wood, S.J., Wellard, R.M., Harrison, B.J., Fornito, A., Pujol, J., Velakoulis, D., Pantelis, C., 2008. Anterior cingulate glutamate-glutamine levels predict symptom severity in women with obsessive-compulsive disorder. Aust N Z J Psychiatry 42, 467–477.